Complex-Source-Point Beam Scattering by a Thin High-Contrast Dielectric Disk

Mikhail V. Balaban*, Ronan Sauleau+, Alexander I. Nosich*

*Institute of Radio-physics and Electronics NASU, Ul. Proskury, 12, Kharkov 61085, Ukraine
mikhail.balaban@gmail.com, alex@emt.kharkov.ua

+IETR, Universite de Rennes 1, Rennes, France
ronan.sauleau@univ-rennes1.fr

***Abstract*— In this paper, we consider the scattering of a complex-source-point beam by a thin high-contrast dielectric disk. To find the solution of the problem, we use analytical-numerical method which is based on the generalized boundary conditions, dual integral equations, and the method of analytical regularization. We present the normalized radiated and absorbed powers as functions of the electrical radius of the disk and far field radiation patterns of the total field at resonance points.**

I. Introduction

Electromagnetic wave scattering by a thin dielectric disk is an interesting problem because of many reasons: such a disk is met as a part of dielectric antennas [1]; it is used as a simplified model of a tree leave [2], thin few-micron radius disks are used as resonators of semiconductor lasers with ultralow thresholds [3], this problem can be simulate the spontaneous emission of light in the presence of a disk-shape nanosize dielectric particle [4], etc.

Many high-frequency approximations and direct computational methods have been used for this problem analysis. However, approximate techniques are commonly applicable if the size of the disk is much larger then the free-space wavelength. Direct computational methods based on the finite differences on time domain have some problems like large-size matrices to be inverted, low convergence of solution, and hence huge computational time. Here we use the method of spectral domain integral equations (IEs). It is based on the dual IEs formulation [5] and the method of analytical regularization [6]. This method has been presented in [7].

II. Modeling

A. Problem Statement

Consider the problem of diffraction of a given time-harmonic electromagnetic field by a thin high-contrast dielectric disk of radius a and thickness τ. Introduce dimensionless cylindrical coordinates $(\rho = r/a, \varphi, \zeta = z/a)$ with origin in the center of the disk. Assume that the incident field is the field of a complex Huygens element (HE) which is the sum of the complex electrical dipole (ED) and magnetic dipole (MD) located at the complex point $d = d_1 + id_2$ perpendicularly each other (Fig. 1). Denote the total field as a sum of the scattered and incident field: $E = E_{in} + E_{sc}$, $H = H_{in} + H_{sc}$ and demand it to satisfy the homogeneous Maxwell equations out of the HE aperture and the disk. Besides, we shrink the disk thickness to zero and introduce

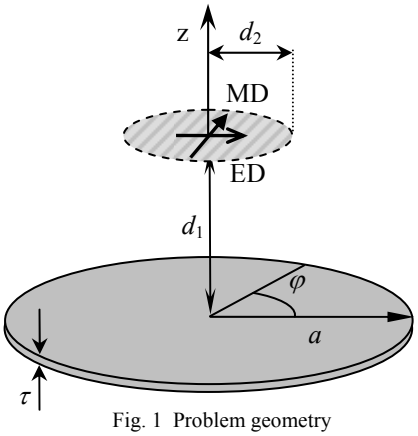

Fig. 1 Problem geometry

the generalized boundary conditions (where the real thickness of the disk τ is included as a parameter) at the median section [8],

$$\left(\vec{E}_{tg}^{+} + \vec{E}_{tg}^{-}\right) = 2Z_0 R \cdot \vec{n} \times \left(\vec{H}_{tg}^{+} - \vec{H}_{tg}^{-}\right),$$
$$\left(\vec{H}_{tg}^{+} + \vec{H}_{tg}^{-}\right) = -2Z_0^{-1} Q \cdot \vec{n} \times \left(\vec{E}_{tg}^{+} - \vec{E}_{tg}^{-}\right). \quad (1)$$

Here, R and Q are the electric and magnetic resistivities given as $R = iZ/2\cot\left(\sqrt{\varepsilon_r \mu_r} k\tau/2\right)$, $Q = R/Z^2$ if $k\tau \ll 1$ and $|\varepsilon_r \mu_r| \gg 1$, Z_0 is the free-space impedance, Z is the relative impedance of the disk material, $k = \omega/c$ is the wavenumber, ε_r and μ_r are the relative permittivity and permeability, respectively. On the rest part of the disk plane the components of the total field are continuous. Also, the scattered field must satisfy the 3D radiation condition and the edge condition [7].

B. Field Components Representation

To obtain field component representations, assume that they are continuous everywhere in the free space except the plane $(\zeta = \xi)$ and satisfy the homogeneous Maxwell equations in doubly-connected domain $\Omega = \Omega^+ \bigcup \Omega^- = \mathbb{R}^3 \setminus \{\zeta = \xi\}$. Then each z-component satisfies Helmholtz equation $\Delta u + (ka)^2 u = 0$ in Ω and can be presented in terms of scalar Fourier-Bessel transform:

$$\begin{pmatrix} E_z^{\mathrm{sgn}(\zeta-\xi)} \\ Z_0 H_z^{\mathrm{sgn}(\zeta-\xi)} \end{pmatrix} = \sum_{m=-\infty}^{\infty} e^{im\varphi} \int_0^{\infty} e^{i\gamma(\kappa)|\zeta-\xi|} J_m(\kappa\rho) \begin{pmatrix} \kappa e_{m,z}^{\mathrm{sgn}(\zeta-\xi)}(\kappa) \\ \kappa h_{m,z}^{\mathrm{sgn}(\zeta-\xi)}(\kappa) \end{pmatrix} d\kappa \quad (2)$$

and tangential to the disk components in terms of the vector Fourier-Bessel transform (3) and (4).

$$\begin{pmatrix} E_r^{\mathrm{sgn}(\zeta-\xi)} \\ -iE_\varphi^{\mathrm{sgn}(\zeta-\xi)} \end{pmatrix} = \sum_{m=-\infty}^{\infty} e^{im\varphi} \int_0^\infty e^{i\gamma(\kappa)|\zeta-\xi|} \overline{H}_m(\kappa\rho) \begin{pmatrix} \mathrm{sgn}(\zeta-\xi)\, i\gamma(\kappa) e_{m,z}^{\mathrm{sgn}(\zeta-\xi)}(\kappa) \\ -ka\, h_{m,z}^{\mathrm{sgn}(\zeta-\xi)}(\kappa) \end{pmatrix} d\kappa \tag{3}$$

$$\begin{pmatrix} Z_0 H_r^{\mathrm{sgn}(\zeta-\xi)} \\ -iZ_0 H_\varphi^{\mathrm{sgn}(\zeta-\xi)} \end{pmatrix} = \sum_{m=-\infty}^{\infty} e^{im\varphi} \int_0^\infty e^{i\gamma(\kappa)|\zeta-\xi|} \overline{H}_m(\kappa\rho) \begin{pmatrix} \mathrm{sgn}(\zeta-\xi)\, i\gamma(\kappa) h_{m,z}^{\mathrm{sgn}(\zeta-\xi)}(\kappa) \\ ka\, e_{m,z}^{\mathrm{sgn}(\zeta-\xi)}(\kappa) \end{pmatrix} d\kappa \tag{4}$$

Here, $\gamma(\kappa) = \sqrt{(ka)^2 - \kappa^2}$ is the complex valued function with the chosen branch $\mathrm{Re}(\gamma(\kappa)) \ge 0$, $\mathrm{Im}(\gamma(\kappa)) \ge 0$ and

$$\overline{H}_m(\kappa\rho) = \begin{pmatrix} J'_{|m|}(\kappa\rho) & mJ_{|m|}(\kappa\rho)/(\kappa\rho) \\ mJ_{|m|}(\kappa\rho)/(\kappa\rho) & J'_{|m|}(\kappa\rho) \end{pmatrix} \tag{5}$$

is vector Hankel transform. Note that thus presented fields components satisfy radiation condition of Silver-Muller automatically.

C. Basic Equations

Substitute the incident and scattered field components which are expressed like (3)-(4) into the generalized boundary conditions (1) and satisfy field continuity condition outside the disk one can obtain the set of coupled dual IEs (9), (10).
Here

$$\begin{aligned} u_m^{sc,\pm}(\kappa) &= \left(e_{m,z}^{sc,+}(\kappa) \pm e_{m,z}^{sc,-}(\kappa)\right)/2, \\ v_m^{sc,\pm}(\kappa) &= \left(h_{m,z}^{sc,+}(\kappa) \pm h_{m,z}^{sc,-}(\kappa)\right)/2 \end{aligned} \tag{6}$$

are functions to be found, and

$$\begin{aligned} u_m^{in,-}(\kappa) &= -\mathrm{sgn}(d_1) e^{i\gamma(\kappa)\left(|d_1| + i\,\mathrm{sgn}(d_1) d_2\right)} e_{m,z}^{in,-\mathrm{sgn}(d_1)}(\kappa), \\ v_m^{in,+}(\kappa) &= e^{i\gamma(\kappa)\left(|d_1| + i\,\mathrm{sgn}(d_1) d_2\right)} h_{m,z}^{in,-\mathrm{sgn}(d_1)}(\kappa) \end{aligned} \tag{7}$$

are given incident-field functions. In the considered case, only the functions with $m = \pm 1$ are not equal to zero, i.e.

$$\begin{aligned} e_{-1,z}^{in,\pm} &= e_{1,z}^{in,\pm} = \kappa\gamma^{-1}(\kappa) \pm i\kappa(ka)^{-1}, \\ -h_{-1,z}^{in,\pm} &= h_{1,z}^{in,\pm} = \kappa\gamma^{-1}(\kappa) \mp i\kappa(ka)^{-1}. \end{aligned} \tag{8}$$

Thus our aim is to find two pairs of unknown functions $(u_*^{sc,-}, v_*^{sc,+})$ and $(v_*^{sc,-}, u_*^{sc,+})$ for $m = \pm 1$. To find the solutions of (9), (10) we, first of all, reduce them to a set of Fredholm second kind IEs by the following semi-inversion procedure which is presented in details in [7]:

1. Integrate the set of coupled dual IEs and "decouple" them by introducing two unknowns are constants of integration. Obtain two sets of dual IEs.
2. Apply the scalar Hankel integral transform and Titchmarsh-type formula to invert the most singular part of the integral operators of the dual IEs. Obtain Fredholm second kind IEs on the (0,∞) interval.
3. Satisfy the edge condition (or the condition of local integrability of power) to find the additional equations for the constants of integration.

Finally we obtain the IEs (11)-(14) for the first pair of unknowns $u_{\pm1}^{sc,-}(\lambda)$ and $v_{\pm1}^{sc,+}(\lambda)$. One can find the similar IEs for the second pair by substitution to (11)-(14) of Q instead of R and $v_{\pm1}^{*,-}(\lambda)$, $-u_{\pm1}^{*,+}(\lambda)$ instead of $u_{\pm1}^{*,-}(\lambda)$, $v_{\pm1}^{*,+}(\lambda)$ respectively.

$$\begin{cases} \displaystyle\int_0^\infty \overline{H}_m(\kappa\rho) \begin{pmatrix} \gamma(\kappa)\left(u_m^{sc,-}(\kappa) + u_m^{in,-}(\kappa)\right) + 2R\,ka\,u_m^{sc,-}(\kappa) \\ ika\left(v_m^{sc,+}(\kappa) + v_m^{in,+}(\kappa)\right) + 2Ri\,\gamma(\kappa) v_m^{sc,+}(\kappa) \end{pmatrix} d\kappa = \overline{0} & (\rho < 1) \\ \displaystyle\int_0^\infty \overline{H}_m(\kappa\rho) \begin{pmatrix} ika\,u_m^{sc,-}(\kappa) \\ -\gamma(\kappa) v_m^{sc,+}(\kappa) \end{pmatrix} d\kappa = \overline{0} & (\rho > 1) \end{cases} \tag{9}$$

$$\begin{cases} \displaystyle\int_0^\infty \overline{H}_m(\kappa\rho) \begin{pmatrix} \gamma(\kappa)\left(v_m^{sc,-}(\kappa) + v_m^{in,-}(\kappa)\right) + 2Q\,ka\,v_m^{sc,-}(\kappa) \\ -\left(ika\left(u_m^{sc,+}(\kappa) + u_m^{in,+}(\kappa)\right) + 2Qi\,\gamma(\kappa) u_m^{sc,+}(\kappa)\right) \end{pmatrix} d\kappa = \overline{0} & (\rho < 1) \\ \displaystyle\int_0^\infty \overline{H}_m(\kappa\rho) \begin{pmatrix} ika\,v_m^{-}(\kappa) \\ \gamma(\kappa) u_m^{+}(\kappa) \end{pmatrix} d\kappa = \overline{0} & (\rho > 1) \end{cases} \tag{10}$$

$$u_{\pm1}^{sc,-}(\lambda) = i\int_0^\infty \kappa^{-1} \left(\left(w(\kappa) + 2Rka\right) u_{\pm1}^{sc,-}(\kappa) + \gamma(\kappa)\, u_{\pm1}^{in,-}(\kappa)\right) S_{1/2}(\kappa,\lambda)\, d\kappa - iA_{\pm1}^l \frac{2\sqrt{2}}{\sqrt{\pi}} \frac{J_{3/2}(\lambda)}{\lambda^{1/2}} \tag{11}$$

$$\gamma(\lambda) v_{\pm1}^{sc,+}(\lambda) = -\frac{ka}{2R} \lambda^{1/2} \int_0^\infty \kappa^{-1/2} \left(v_{\pm1}^{sc,+}(\kappa) + v_{\pm1}^{in,+}(\kappa)\right) S_2(\kappa,\lambda) d\kappa \mp 2D_{\pm1}^r J_1(\lambda) \tag{12}$$

$$\frac{4}{3} A_{\pm1}^l - (ka)^{-1} D_{\pm1}^r = \sqrt{\frac{2}{\pi}} \int_0^\infty \kappa^{-3/2} \left(\left(w(\kappa) + 2Rka\right) u_{\pm1}^{sc,-}(\kappa) + \gamma(\kappa)\, u_{\pm1}^{in,-}(\kappa)\right) J_{3/2}(\kappa)\, d\kappa \tag{13}$$

$$\frac{i}{2R} A_{\pm1}^l + D_{\pm1}^r = \pm \frac{ka}{2R} \int_0^\infty \kappa^{-1} \left(v_{\pm1}^{sc,+}(\kappa) + v_{\pm1}^{in,+}(\kappa)\right) J_1(\kappa) d\kappa \tag{14}$$

D. Numerical Solution

Favourable features of the Fredholm second kind IEs guarantee the uniqueness and existence of their solutions and convergence of numerical algorithm based on any reasonable discretization scheme. In our work we use the following one:

4. Introduce the truncation number $N \geq ka + 1$ and truncate the interval of integration to $(0,N)$.
5. Apply the Nystrom method with the Gauss-type higher-order quadratures to discretize IEs on the $(0,N)$ interval. Find the unknowns at the grid points by inverting the matrix analog of IEs .
6. Find the unknown functions on the $(0,\infty)$ interval by substitution of the set of found values into the Fredholm second kind IEs.

Fig. 2 shows the dependences of the relative truncation error on the truncation number. One can see a typical behaviour of this error which corresponds to the features of the Fredholm second kind IEs.

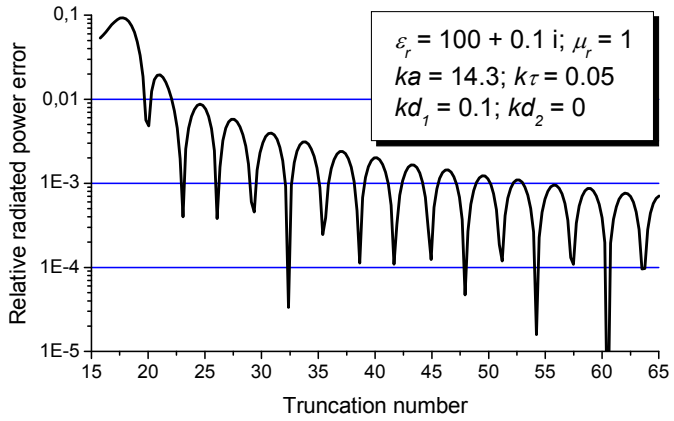

Fig. 2 Relative truncation error vs. trunc. number

III. Results and Discussion

To show some results of the study we consider a high-contrast dielectric disk with $\varepsilon = 100 + 0.1i$ (as an example) and put HE at the point $kd_1 = 0.1$. Note that the HE field is a wave beam with the width determined by the normalized parameter kd_2. We consider three values of kd_2 = 0,0;-0.5;-1.0. The radiation patterns of such HEs are presented in Fig. 3. In Fig. 4 and Fig. 5, we present the normalized radiated and absorbed powers as functions of the normalized radius of the disk ka. One can see the resonance nature of these values due to the radial modes of the disk. In Fig. 6, we present the radiation patterns of the total field (in two principal planes) at three resonance points marked in Fig. 4. Note that in the case of the source point having non-zero imaginary part ($kd_2 \neq 0$) there is another non-resonance maximum on the radiated power curve. It corresponds to the situation where the aperture radius of the complex HE equals to the radius of the disk ($kd_2 = ka$).

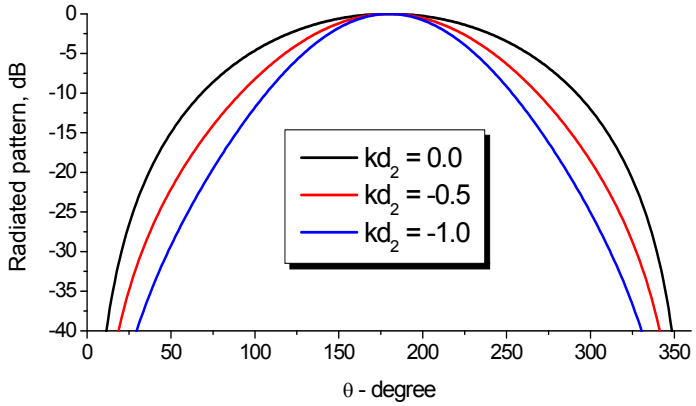

Fig. 3 Radiation pattern of the complex HE

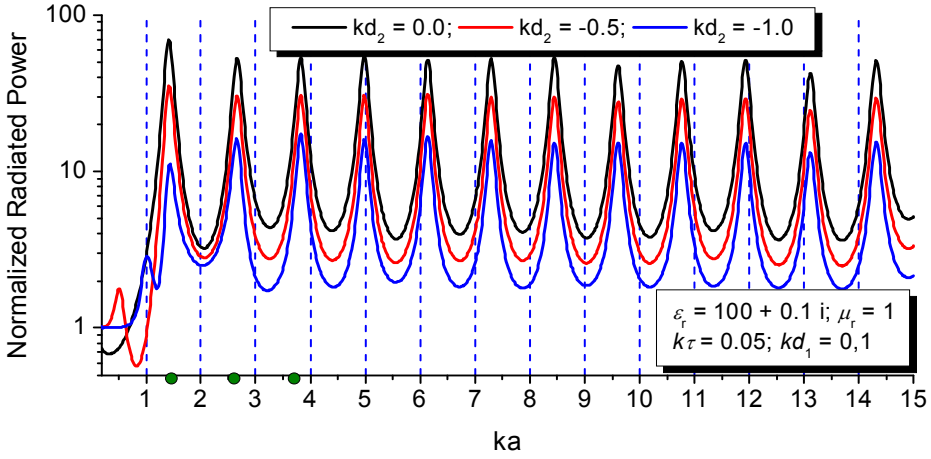

Fig. 4 Normalized radiated powers as functions of the disk radius ka

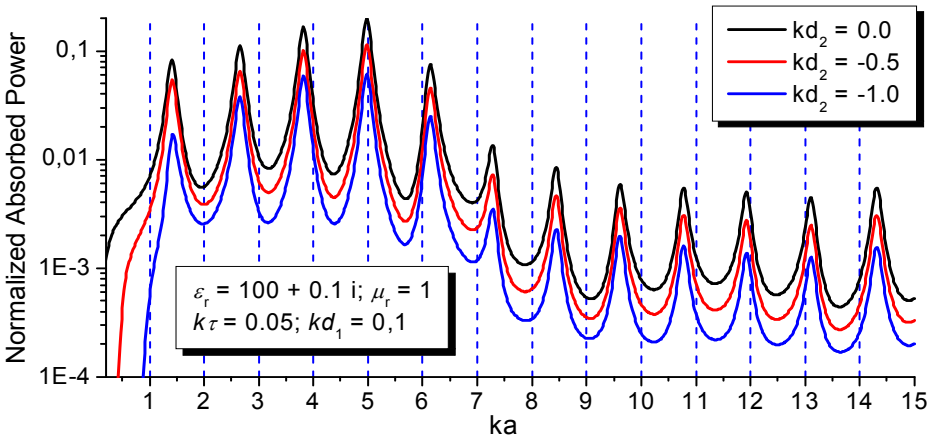

Fig. 5 Normalized absorbed powers as functions of the disk radius ka

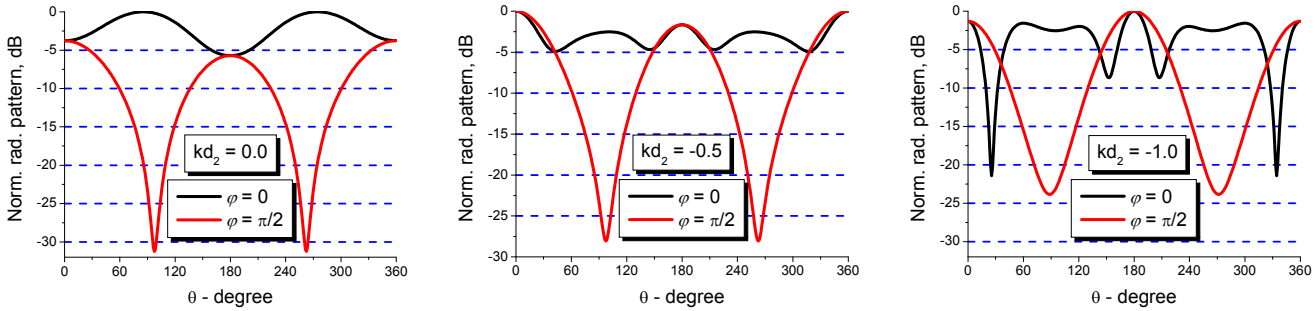

(a) (b) (c)

Fig 6 Radiation patterns of the total field in the resonances marked in Fig. 4 above

IV. Conclusions

We present the modelling method and fast convergent numerical algorithm for the analysis of a complex-source-point beam 3-D scattering by a thin high-contrast dielectric disk. Starting from the Maxwell equations and two-side generalized boundary conditions, we reduce the problem to a set of Fredholm second kind integral equations which we solve numerically. We show the plots of the normalized radiated and absorbed powers as functions of the normalized radius of the disk and present the radiation patterns of the total field at some resonance points.

This study is a first step to the simulation of the full wave scattering by varying-thickness disks, i.e. mm-wave and THz lenses, and finite collections of uniform disks, for instance, Yagi-Uda like arrays.

Acknowledgments

This work was supported by the National Academy of Sciences of Ukraine via the State Target Program "Nanotechnologies and Nanomaterials", and the European Science Foundation via the Networking Programme "Newfocus".

References

[1] N. Y. Bliznyuk, A. I. Nosich, "Numerical analysis of a lossy circular microstrip antenna," *Telecommunications and Radio Engineering*, vol. 55, no. 8, pp. 15-23, 2001.

[2] I. S. Koh, K. Sarabandi, "A new approximate solution for scattering by thin dielectric disks of arbitrary size and shape," *IEEE Trans. Antennas Propagation*, vol. 53, no. 6, pp. 1920-1926, 2005.

[3] N. C. Frateschi and A. F. J. Levi, "Resonant modes and laser spectrum of microdisk lasers," *Appl. Phys. Lett.*, vol. 66, no. 22, pp. 2932–2934, 1995.

[4] L. Rogobete, C. Henkel, "Spontaneous emission in a subwavelenght environment by boundary integral equations," *Phys. Rev. A.* vol. 70, no 6, pp. 3815-3824, 2004.

[5] W. C. Chew, J. A. Kong, "Resonance of axially symmetric modes in microstrip disk resonators," J. Math. Phys., Vol. 21, No. 3, p. 582, 1980.

[6] A .I. Nosich, "Method of analytical regularization based on the static part inversion in wave scattering by imperfect thin screens", *J. Telecommunications and Information Technology*, Warsaw: NIT Press, no 3, pp. 72-79, 2001.

[7] M. V. Balaban, R. Sauleau, T. M. Benson, A. I. Nosich, "Dual integral equations technique in electromagnetic wave scattering by a thin disk," *Progress in Electromagnetic Research B*, vol. 16, pp. 107-126, 2009.

[8] E. Bleszynski, M. Bleszynski, T Jaroszewicz, "Surface-integral equations for electromagnetic scattering from impenetrable and penetrable sheets," *IEEE Antennas Propag. Mag.*, vol. 35, pp. 14-24, 1993.